Expression of a chimeric antigen receptor specific for donor HLA class I enhances the potency of

human regulatory T cells in preventing human skin transplant rejection

Authors: Dominic A. Boardman[1,2], Christina Philippeos[3], Gilbert O. Fruhwirth[4], Mohammad A. A.

Ibrahim[5,6], Rosalind F. Hannen[7], Dianne Cooper[8], Federica M. Marelli-Berg[8], Fiona M. Watt[2,3], Robert

I. Lechler[1,2]†, John Maher[2,5,9]†, Lesley A. Smyth[1,10]†, Giovanna Lombardi[1,2]*†

Affiliations

1   MRC Centre for Transplantation, King's College London, Guy's Hospital, London SE1 9RT, UK

2   NIHR Biomedical Research Centre, Guy's & St Thomas' NHS Foundation Trust & King's College

    London, Guy's Hospital, London SE1 9RT, UK

3   Centre for Stem Cells & Regenerative Medicine, King's College London, Guy's Hospital, London

    SE1 9RT, UK

4   Department of Imaging Chemistry and Biology, Division of Imaging Sciences and Biomedical

    Engineering, King's College London, St.Thomas' Hospital, London SE1 7EH, UK

5   Department of Clinical Immunology and Allergy, King's College London, King's College

    Hospital, London SE5 9RS, UK

6   Division of Asthma, Allergy & Lung Biology, King's College London, Guy's Hospital, London SE1

    9RT, UK

7   Centre for Cell Biology & Cutaneous Research, Bart's and The London School of Medicine and

Dentistry, Queen Mary University of London, London E1 2AT, UK

8   William Harvey Research Institute, Bart's and The London School of Medicine, Queen Mary

University of London, London EC1M 6BQ, UK

9   CAR Mechanics Group, Division of Cancer Studies, King's College London, Guy's Hospital,

London SE1 9RT, UK

10 School of Health, Sport and Bioscience, Stratford Campus, University of East London, London

E15 4LZ, UK

* To whom correspondence should be addressed:

Prof. Giovanna Lombardi

giovanna.lombardi@kcl.ac.uk

† Co-last author

Running title: MHC I-allospecific CAR Treg graft protection

Abbreviations:

ANOVA	Analysis of variance
APC	Antigen presenting cell
B-LCL	B-lymphoblastoid cell line
bp	Base pair
BRG	BALB/c Rag2$^{-/-}$γ$_c$$^{-/-}$
CAR	Chimeric antigen receptor
CLA	Cutaneous lymphocyte antigen

cpm	Counts per minute
eGFP	Enhanced green fluorescent protein
ELISA	Enzyme-linked immunosorbent assay
FACS	Fluorescence-assisted cell sorting
FOXP3	Factor forkhead-box protein 3
GMP	Good medical practice
GvHD	Graft-versus-host disease
HUVEC	Human umbilical cord endothelial cell
i.p.	Intraperitoneal
i.v.	Intravenous
MTT	3-(4,5-Dimethylthiazol-2-yl)-2,5-Diphenyltetrazolium Bromide
OCT	Optimal cutting temperature
PBMC	Peripheral blood mononuclear cell
RAG	Recombination activating gene
scFv	Single-chain variable fragment
SD	Standard deviation
SE	Standard error of the mean
Teff	Effector T cell
Treg	Regulatory T cells

ABSTRACT

Regulatory T cell (Treg) therapy using recipient-derived Tregs expanded *ex vivo* is currently being investigated clinically by us and others as a means of reducing allograft rejection following organ transplantation. Data from animal models has demonstrated that adoptive transfer of allospecific Tregs offers greater protection from graft rejection compared to polyclonal Tregs. Chimeric antigen receptors (CAR) are clinically-translatable synthetic fusion proteins which can redirect the specificity of T cells towards designated antigens. We used CAR technology to redirect human polyclonal Tregs towards donor-MHC class I molecules which are ubiquitously expressed in allografts. Two novel HLA-A2-specific CARs were engineered: one comprising a CD28-CD3ζ signalling domain (CAR) and one lacking an intracellular signalling domain (ΔCAR). CAR Tregs were specifically activated and

significantly more suppressive than polyclonal or ΔCAR Tregs in the presence of HLA-A2, without eliciting cytotoxic activity. Furthermore, CAR and ΔCAR Tregs preferentially transmigrated across HLA-A2-expressing endothelial cell monolayers. In a human skin xenograft transplant model, adoptive transfer of CAR Tregs alleviated the alloimmune-mediated skin injury caused by transferring allogeneic PBMCs more effectively than polyclonal Tregs. Our results demonstrated that the use of CAR technology is a clinically applicable refinement of Treg therapy for organ transplantation.

INTRODUCTION

The long-term benefits of organ transplantation are hindered by graft rejection (1-5), a detrimental process driven by alloreactive T cells which recognise donor MHC antigens via the direct, indirect and semi-direct pathways of allorecognition (3, 6). Current immunosuppressive regimens target the direct pathway and reduce acute allograft rejection (7) but are associated with severe side-effects (8) and do not effectively prevent chronic rejection (2, 9), thus the half-life of allografts remains limited to

10-15 years (10, 11).

Thymus-derived regulatory T cells (tTregs) are immunosuppressive T cells with a fundamental role in the maintenance of tolerance *in vivo* (12-15). These cells are characterised in humans as CD4$^+$CD25^{hi}CD127^{lo} and constitutively express the transcription factor forkhead-box protein 3 (FOXP3) (7, 12, 16). In rodent models, Tregs significantly prolong the survival of skin (17-19) and heart (4) allografts and in humans, correlations between the proportion of Tregs within allografts and graft survival have been observed (20-22). With the safety of Treg therapy having been demonstrated in the contexts of graft-versus-host disease (GvHD) (23-26) and Type I diabetes (27, 28), we are conducting Phase I/II clinical trials to investigate the therapeutic potential of adoptive

polyclonal Treg therapy to promote tolerance in kidney (the ONE Study: NCT02129881) and liver

(ThRIL: NCT02166177) transplant recipients (29, 30).

However, we (4, 17, 19, 31), and others (32, 33), have demonstrated in animal models that

allospecific Tregs are superior to polyclonal Tregs at reducing graft rejection, upon adoptive transfer.

Murine Tregs expanded with allogeneic antigen presenting cells (APC) (direct allospecificity) and/or

transduced to express an allospecific TCR (indirect allospecificity) prolonged graft survival

significantly more effectively than polyclonal Tregs. These findings were confirmed using human

Tregs expanded with allogeneic dendritic cells (19) and B cells (31, 34) in human skin xenograft

transplant models. As such, clinical trials are assessing the safety and efficacy of Tregs with direct

allospecificity in kidney (DART: NCT02188719) and liver (delta: NCT02188719 and NCT01624077)

transplant recipients. Here, we investigated whether allospecificity may be conferred onto Tregs

using chimeric antigen receptors (CAR) (35).

CARs are synthetic fusion proteins capable of redirecting the specificity of T cells towards desired

antigens. Classical CARs comprise an extracellular antigen-targeting moiety which binds a specific

antigen in an MHC-independent manner and a series of customised intracellular TCR and co-

stimulatory signalling domains. As such, CARs translate the binding of specific antigens into the

activation of desired signalling cascades (36). CARs are primarily used clinically to generate tumour

antigen-specific T cells (37-43). However, pre-clinical studies have shown the efficacy of CAR-

modified Tregs for the treatment of colitis (16, 44, 45) and multiple sclerosis (46). The functionality

of CARs has also been demonstrated in human Tregs (47, 48), most recently as a means of protecting

against xeno-GvHD (49). However, to date, nobody has demonstrated the capacity of CAR Tregs to

protect from solid transplant rejection.

In this study, we applied CAR technology to generate allospecific Tregs with the aim of promoting

organ transplant tolerance. We redirected human CD4$^+$CD25$^+$CD127^{lo}FOXP3$^+$ Tregs towards an MHC

class I molecule (HLA-A2), an alloantigen which is ubiquitously expressed in an allograft, with the

hypothesis that they would be more potent than polyclonal Tregs at protecting from graft rejection, upon adoptive transfer.

MATERIALS AND METHODS

CAR generation

A previously described (50) HLA-A2-specific single chain variable fragment (scFv) sequence (3PB2 V_H and DPK1 V_L) was validated by immunoprecipitation (data not shown) and cloned upstream of i) a 9E10 cMyc epitope; ii) a human CD28 hinge/transmembrane domain; iii) a human CD28-CD3ζ signalling domain; and iv) an enhanced green florescent protein (eGFP) open reading frame (ORF) in a second generation pLNT/SFFV lentiviral plasmid (provided by Prof. Adrian Thrasher; UCL, London, UK). A truncated CAR (ΔCAR) was generated by removing the CD28-CD3ζ signalling domain from the full-length CAR-eGFP fusion. All plasmids were verified by sequencing (Beckman Coulter Genomics).

Human CD4$^+$CD25$^+$ Treg and CD4$^+$CD25$^-$ Teff isolation and culture

Anonymised healthy donor peripheral blood was obtained from the National Blood Service (NHS Blood and Transplantation, Tooting, London, UK) with informed consent and ethical approval (Institutional Review Board of Guy's Hospital; reference 09/H0707/86). CD4$^+$ T cells were enriched using RosetteSep™ (StemCell Technologies) after which CD4$^+$CD25$^+$ Tregs and CD4$^+$CD25$^-$ Teffs were separated using CD25 MicroBeads II (Miltenyi Biotec).

Tregs/Teffs were activated with anti-CD3/CD28 beads (1:1 bead:cell ratio; Thermo Fisher Scientific) and cultured in X-vivo 15 (Lonza) supplemented with 5% human AB serum (BioSera). Treg were cultured with 100 nM rapamycin (LC-Laboratories) and 1,000 U/mL recombinant IL-2 (Proleukin-Novartis) whilst Teffs were cultured with 100 U/mL IL-2 only.

Flow cytometry and cell sorting

Cells were stained in phosphate buffered saline (PBS) supplemented with 1% heat-inactivated foetal calf serum (FCS) and 5 mM EDTA (all from Thermo Fisher Scientific) using fluorescently-conjugated antibodies specific for HLA-A2 (BB7.2), CD4 (OKT4), FOXP3 (PCH101), CD39 (eBioA1), CD69 (H1.2F3) (all from eBioscience), CD25 (4E3 or 2A3), CTLA-4 (BNI3) (all from BD Biosciences) CD127 (A019D5), CCR4 (L291H4), CCR9 (L053E8), CCR10 (5688-5), CD62L (DREG-56), integrin β7 (FIB504), CLA (HECA-452), HLA-DR (all from BioLegend), HLA-A2 (REA142) (Miltenyi-Biotec) and HLA class I (Tu149) (Thermo Fisher Scientific). Cells were stained with PE-conjugated HLA-A*0201/CINGVCWTV and HLA-B*0702/DPRRRSRNL dextramers (Immudex) provided by Dr. Marc Martinez-Llordella; KCL, London, UK. Dead cells were excluded using live/dead near-IR staining (Thermo Fisher Scientific). Intracellular staining was performed using the eBioscience Fix/Perm kit. Cells were acquired and sorted using an LSRFortessa II and FACSAria II (BD), respectively. Data was analysed using FlowJo 7 or 10 (Tree Star).

Immortalised cell line culture

HEK293T, MCF-7, and T-47D epithelial cells were grown in DMEM-based media. B-Lymphoblastoid cell lines (B-LCL) and K562s (donated by Dr. Marc Martinez-Llordella) were grown in RPMI-based media. All culture medias were supplemented with 10% heat-inactivated FCS, 100 units/mL penicillin, 100 µg/mL streptomycin and 2 mM L-glutamine (all from Thermo Fisher Scientific). HLA-transfected K562 cultures were supplemented with 5 µg/mL neomycin (Thermo Fisher Scientific). All cells were grown at 37°C in the presence of 5% (v/v) CO_2.

Lentivirus production and Treg/Teff transduction

HEK293T cells were co-transfected with pLNT/SFFV-CAR-eGFP or pLNT/SFFV-ΔCAR-eGFP (Figure 1A), pΔ8.91 and pCMV-VSV-G plasmids at a mass ratio of 4:3:1 using polyethylenimine (3:1 PEI:DNA w/w;

Sigma-Aldrich). Viral supernatant was harvested 48-56 hours post-transfection and lentiviral particles were concentrated using PEG-it™ (System Biosciences). Tregs/Teffs were transduced in RetroNectin-treated plates (50 µg/µL; Takara Bio Inc.) 3 days post-isolation using 4-fold concentrated viral supernatant. eGFP$^+$ cells were purified by FACS 7 days post-transduction.

T cell/epithelial cell co-culture

Teffs/Tregs were co-cultured overnight with confluent MCF-7 or T-47D cell monolayers. Culture supernatants were collected to measure IL-2, interferon (IFN)γ and IL-10 production by cytokine-specific enzyme-linked immunosorbent assays (ELISA) (eBioscience). Monolayers were washed and the viability of the monolayer cells was determined by 3-(4,5-Dimethylthiazol-2-yl)-2,5-Diphenyltetrazolium Bromide (MTT) assay. Absorbance was measured at 560 nm. Results are shown as percent viability relative to monolayers cultured alone.

Suppression assays

Tregs were co-cultured with autologous CD4$^+$CD25$^-$ Teff responders which were labelled with CellTrace Violet (CTV; Thermo Fisher Scientific) and activated with anti-CD3/CD28 beads (1:40 bead:cell ratio) or irradiated (12,000 cGy) allogeneic B-LCLs (3:1 T:B-LCL ratio); DBB (HLA-A2$^+$DR7$^+$), MOU (HLA-A2$^-$DR7$^+$), SPO (HLA-A2$^+$DR11$^+$) and BM21 (HLA-A2$^-$DR11$^+$). Teff CTV dilution was measured after 5 days using flow cytometry. Results are shown as percent suppression (inverse of percent Teff proliferation) relative to Teffs cultured alone.

In vitro flow chamber assay

Primary human umbilical vein endothelial cells (HUVECs) were isolated by collagenase digestion using ethically-approved protocols (East London & The City Local Research Ethics Committee reference 05/Q0603/34 ELCHA). HUVECs were stimulated with 15 ng/mL IFNγ for 72 hours (R&D) prior to experimentation and seeded in μ-Slides VI 0.4 (Ibidi) coated with 0.5% bovine gelatin. Tregs were suspended at $1x10^6$ cells/mL in PBS (with Ca^{2+} and Mg^{2+}) and flowed across HUVEC layers using a shear stress of 1 dyn/cm^2. The number of Tregs which migrated in 10 second frames was assessed.

Animals

BALB/c recombination activating gene (RAG)$2^{-/-}\gamma_c^{-/-}$ (BRG) mice were maintained under sterile conditions (Biological Services Unit, New Hunt's House, King's College London). All procedures were performed in accordance with all legal, ethical and institutional requirements (PPL70/7302).

Human skin xenograft transplant model

Human skin was obtained from routine surgical procedures with informed consent and ethical approval (Guy's and St. Thomas' NHS Foundation Trust and King's College London; reference 06/Q0704/18). Donor HLA-A2 expression was determined by flow cytometry, staining skin-derived cells obtained by collagenase digestion (100 μg/mL, Sigma-Aldrich). 1.5 cm^2 split-thickness skin grafts were transplanted onto 10-11 week old recipient BRG mice as previously described (19) and mice were administered 100 μg anti-mouse Gr-1 (BioXCell) intraperitoneally every 3-4 days. After 5-6 weeks (Figure S4), mice were injected intravenously with $5x10^6$ PBMCs ± $1x10^6$ Tregs. Skin grafts were harvested for histological analysis 5 weeks following PBMCs/Tregs transfer.

Histological analysis of human skin

Skin grafts were frozen in optimum cutting temperature (OCT) (Thermo Fisher Scientific). 8 or 16 µm thick sections were fixed in 4% paraformaldehyde, blocked with a mixture of 10% donkey serum, 0.1% fish skin gelatin, 0.1% Triton X-100 and 0.5% Tween-20 (all from Sigma-Aldrich) in PBS and stained with the following antibodies: anti-human CD3 (polyclonal rabbit, DAKO), anti-FOXP3 (236A/E7, Abcam), anti-CD45 (HI30, eBioscience), anti-involucrin (CY5, Sigma-Aldrich), anti-human CD31 and Ki67 (both polyclonal rabbit, Abcam). Sections were stained with secondary donkey anti-mouse Alexa Fluor®555 and anti-rabbit Alexa Fluor®488 or Alexa Fluor®647 antibodies with 4-6-diamidino-2-phenylindole (DAPI) (all from Thermo Fisher Scientific) and mounted with Fluorescence Mounting Medium (DAKO). Maximum intensity projection images consisting of 10 z-stacks (1.1 µm apart) were acquired at x20 magnification using a C2+ point scanning confocal microscope (Nikon) and analysed/quantified with NIS Elements and FIJI imaging software (51).

Statistical analysis

Data shown is mean ± standard error (SEM) or mean ± standard deviation (SD). Statistical significance was determined using two-tailed paired Student's t-tests or analysis of variance (ANOVA) with the Tukey multiple comparison post-hoc test. *=p<0.05, **=p<0.01, ***=p<0.001 and ****=p<0.0001.

RESULTS

Generation and validation of a novel HLA-A2-specific CAR

A HLA-A2-specific CAR incorporating a human CD28-CD3ζ signalling domain was generated using a patient-derived HLA-A2-specific scFv sequence (50) (Figure 1A-B). A second generation CAR was

selected based on the superior function of these CARs relative to first generation CARs (52-55) and the importance of CD28 signalling for Treg activation (56). To investigate the importance of this signalling domain, a HLA-A2-specific CAR lacking a CD28-CD3ζ signalling domain (ΔCAR) was also generated (Figure 1A-B). This control was selected, as opposed to a CAR containing a scrambled ectodomain, to ascertain whether the ability of the Tregs to engage HLA-A2 was sufficient to elicit protection *in vivo* or whether Treg activation via the CAR was also necessary.

To confirm the functionality and HLA-A2-specificity of these CARs, polyclonal CD4$^+$CD25$^-$ effector T cells (Teffs) were transduced with VSV-G-pseudotyped lentiviral particles containing the CAR or the ΔCAR constructs with an efficiency of 40-80% (54.3-62.8 ± 11.9%; Figure 1C). eGFP$^+$ Teffs were purified by cell sorting and co-cultured overnight with confluent monolayers of MCF-7 and T-47D cells, breast cancer epithelial cells which differentially expressed HLA-A2 (Figure 1D and (57)). CAR Teffs specifically destroyed HLA-A2$^+$ monolayers but left HLA-A2$^-$ monolayers intact (Figure 1E). Compared to epithelial cells cultured alone, CAR Teffs killed 80.8 ± 4.2% of the HLA-A2$^+$ cells but not the HLA-A2$^-$ cells (Figure 1F). Untransduced and ΔCAR Teffs exhibited no detectable level of cytotoxicity. High levels of IL-2 (Figure 1G) and IFNγ (Figure 1H) were also produced by the CAR Teffs during co-culture with HLA-A2$^+$ cells. These results demonstrated that CAR expression by T cells mediated specific recognition of HLA-A2 antigens resulting in Teff activation, cytotoxicity and cytokine production.

Human CD4$^+$CD25$^+$ Tregs maintained their phenotype and function following lentiviral CAR transduction

Having validated the CARs in Teffs, we next assessed whether lentiviral transduction influenced the phenotype and/or suppressive capacity of human Tregs. CD4$^+$CD25$^+$ Tregs were enriched using GMP-compatible protocols (58) from the peripheral blood of healthy HLA-A2$^-$ donors with a purity of

approximately 90% (89.5 ± 4.4%, n=16; Figure S1A). A high proportion of the cells were FOXP3$^+$ with a low expression of CD127 (Figure S1B). These cells were activated using anti-CD3/CD28 beads and expanded in the presence of 1,000 U/mL recombinant human IL-2 and 100 nM rapamycin (29, 58). Tregs were transduced with the CAR or ΔCAR construct 72 hours post-activation (Figure 2A), with efficiencies of 30-80% (55.1-69.2 ± 20.3%, n=15; Figure 2B). eGFP$^+$ Tregs were purified by flow sorting 7 days post-transduction (Figure 2B) and expanded for an additional 10 days (Figure 2A). All eGFP$^+$ Tregs were shown to have a detectable level of CAR expression on the cell surface (Figure 2B) which facilitated in the specific recognition of a HLA-A2-based dextramer but not an irrelevant HLA-B7-based dextramer (Figure 2C). Furthermore, engagement of HLA-A2 was shown to specifically activate CAR Tregs but not untransduced or ΔCAR Tregs (Figure 2D and Figure S2).

Following expansion, >95% (95.3-97.8 ± 4.7%) of the transduced Tregs remained eGFP$^+$. These cells exhibited a similar phenotype to untransduced Tregs (Figure 2E and Figure S3A); they remained CD4$^+$CD25$^+$CD127^{lo} with a high proportion expressing FOXP3 (94.2-95.8 ± 7.3%), CTLA-4 (91.3-95.3 ± 3.1%) and CD39 (72.4-81.7 ± 16.3%). Treg expression of specific homing receptors was also unaltered (Figure 2F and Figure S3B). The Tregs expressed the skin homing molecules CCR4 (96.7-98.8 ±3.2%) and cutaneous lymphocyte antigen (CLA) (48.4-51.0 ± 26.4%) but few cells expressed CCR10 (0.6-1.5 ± 0.7%), as previously published (58). All cells expressed CD62L (93.7-95.6 ± 3.9%) and with regards to gut homing, a high proportion expressed integrin β7 (91.7-93.2 ± 5.9%) but few cells expressed CCR9 (1.1-1.7 ± 1.0%).

To assess the suppressive capacity of the Tregs, untransduced, CAR and ΔCAR Tregs were co-cultured with CTV-labelled autologous CD4$^+$CD25$^-$ responder Teffs in the presence of anti-CD3/28 beads for 5 days. At a 1:32 Treg:Teff ratio, untransduced, CAR and ΔCAR Tregs inhibited Teff proliferation by 43.0 ± 4.1%, 44.8 ± 5.4% and 39.4 ± 5.7%, respectively, proving the potency of these cells and indicating that the Treg function following transduction was unaltered.

Taken together, these results demonstrated that human Tregs isolated and expanded with clinically-relevant protocols maintained their phenotype and function following transduction with VSV-G-pseudotyped lentiviral particles.

CAR-mediated alloantigen recognition by human Tregs enhanced their potency

To assess whether CAR Tregs were functionally superior to untransduced (polyclonal) Tregs in the presence of HLA-A2, Tregs were co-cultured with CTV-labelled CD4$^+$CD25$^-$ responder Teffs and allogeneic B-LCLs which differentially expressed HLA-A2 as APCs. The suppressive profile of the polyclonal Tregs cultured with HLA-A2$^+$ and HLA-A2$^-$ B-LCLs was identical (Figure 3A) whilst CAR Tregs inhibited Teff proliferation significantly more effectively (*p*-values 0.0082-1.1x10^{-5}) in the presence of HLA-A2$^+$ B-LCLs, compared to HLA-A2$^-$ B-LCLs (Figure 3B). At a 1:32 and 1:64 Treg:Teff ratio, CAR Tregs inhibited Teff proliferation by 62.8 ± 5.2% and 38.1 ± 3.6%, respectively, in the presence of HLA-A2 but only 35.8 ± 3.5% and 16.9 ± 3.4%, respectively, in the absence of HLA-A2. ΔCAR Tregs were significantly more suppressive in the presence of HLA-A2 at Treg:Teff ratios of 1:2 (*p*=0.041) and a 1:32 (*p*=0.027) (Figure 3C). This minor increase in suppressive ability may have been due to the antigen-targeting moiety of the ΔCAR facilitating an interaction between the ΔCAR Tregs and the HLA-A2$^+$ APCs, bringing the Treg into the vicinity of the Teff:B-LCL interaction.

Tregs can function by secreting granzyme and perforin (59, 60). To exclude the risk of unwanted cytotoxicity, Tregs were co-cultured with confluent monolayers of HLA-A2$^+$ and HLA-A2$^-$ epithelial cells, as previously described (Figure 1). Unlike CAR Teffs, CAR Tregs exhibited no detectable level of cytotoxicity towards the HLA-A2$^+$ cells (Figure 3D). IL-2 secretion was undetectable in all conditions analysed (data not shown) and low levels of IFNγ (221 ± 80 pg/μL; Figure 3E) were produced by CAR Tregs co-cultured with HLA-A2$^+$ monolayers. In contrast, these cells produced significantly high levels of the immunosuppressive cytokine IL-10 (1,055 ± 78 pg/μL) compared to polyclonal Tregs (not

detected) and ΔCAR Tregs (8 ± 1 pg/µL) (Figure 3F), suggesting that *in vivo*, CAR Tregs would contribute to the establishment of an intragraft immunosuppressive milieu in HLA-A2$^+$ allografts.

Given the importance of Treg trafficking *in vivo*, we investigated whether the expression of HLA-A2 by endothelial cells influenced the rate with which CAR Tregs transmigrated (61). Relative to polyclonal Tregs, CAR and ΔCAR Tregs transmigrated through HLA-A2$^+$ endothelial monolayers significantly faster than through HLA-A2$^-$ endothelial monolayers (*p*=0.042; Figure 3G), suggesting a preferential migration into HLA-A2$^+$ target tissues.

Overall, these results demonstrated that compared to polyclonal Tregs, donor-specific CAR Tregs exhibited a greater suppressive capacity in the presence of HLA-A2 without eliciting cytotoxic activity and transmigrated at a faster rate through HUVECs expressing HLA-A2.

CAR-mediated Treg allorecognition conferred a functional advantage in preventing skin graft rejection

We have previously demonstrated the superior efficacy of human Tregs with direct allospecificity over polyclonal Tregs at reducing alloimmune injury in a human skin xenograft transplant model (19, 31). To investigate whether CAR Tregs elicited a similar protective role, the same model was employed (Figure S4). Human skin was obtained from routine abdominal angioplasty surgery and HLA-A2 expression was determined using collagenase-treated skin explants (Figure S5). BRG mice were transplanted with HLA-A2$^+$ skin grafts and following skin engraftment, were injected with allogeneic CD25-depleted HLA-A2$^-$ PBMCs ± autologous Tregs. Mice did not exhibit any signs of GvHD throughout the experiments (Figure S6A). Skin grafts were explanted and analysed histologically for changes in the skin morphology and immune cell infiltration 5 weeks post-PBMC transfer (Figure S4B). Cryosections were stained with haemotoxalin and eosin (Figure S6B) or analysed by immunofluorescence.

Significant alloimmune damage was observed in the grafts of mice which received PBMCs, as demonstrated by a high number of Ki67$^+$ keratinocytes (Figure 4A), a loss of CD31$^+$ blood vessel integrity and loss of the involucrin-expressing epidermal layer (Figure 4B). Grafts of mice treated with PBMCs and Tregs had comparatively fewer Ki67$^+$ keratinocytes (Figure 4A), intact CD31$^+$ blood vessels and a defined involucrin layer (62) (Figure 4B). Quantification of these observations demonstrated that CAR Treg treatment reduced the number of Ki67$^+$ keratinocytes to basal levels, exhibiting significantly more protection than polyclonal Tregs ($p=0.042$) (Figure 4D). Interestingly, in this readout of graft damage, ΔCAR Tregs also mediated superior protection to polyclonal Tregs, although statistical significance was not reached ($p=0.11$). Conversely, when measuring damage in terms of CD31$^+$ blood vessel integrity, CAR Tregs (CD31$^+$ cluster size = 88.9 ± 8.5; $p<0.0001$) mediated protection more effectively than both polyclonal (73.3 ± 8.7; $p=0.017$) and ΔCAR (70.9 ± 10.1; $p=0.026$) Tregs (Figure 4E). Mice which received PBMCs with CAR or ΔCAR Tregs ($p<0.0001$ versus PBMCs alone) had a greater FOXP3:CD3 ratio than mice which received PBMCs with polyclonal Tregs ($p=0.019$). Together, these results suggested that CAR expression facilitated preferential homing and retention of the Tregs in the HLA-A2$^+$ allografts. This localisation to the graft enabled the ΔCAR Tregs to elicit more protection than polyclonal Tregs, likely due to these cells being activated in a TCR-dependent manner through direct allorecognition. However, the protection offered was further improved upon by the CAR Tregs which were activated in both a TCR-dependent (direct allorecognition) and CAR-dependent manner.

In conclusion, CAR-engineered HLA-A2-specific Tregs inhibited alloimmune-mediated injury against HLA-A2$^+$ skin allografts significantly more effectively than polyclonal or ΔCAR Tregs demonstrating the increased potency of these cells *in vivo* and the requirement for Treg signalling to elicit this response.

DISCUSSION

Animal models of transplantation have demonstrated that allospecific Tregs are superior to polyclonal Tregs at protecting from allograft rejection (4, 17, 19, 31-34). Here, we isolated human Tregs using GMP-compatible protocols and used CAR technology to generate donor-MHC class I-allospecific CAR Tregs which were functionally superior to polyclonal Tregs *in vitro* and in a human skin xenograft transplant model. These results demonstrated a promising new direction for clinical trials which are currently assessing the safety and efficacy of polyclonal Treg therapy in kidney (the ONE Study: NCT02129881) and liver (ThRIL: NCT02166177) transplant recipients (29, 30).

Tregs which recognise allo-MHC-peptide complexes (direct allorecognition) and/or allopeptides presented in the context of recipient MHC (indirect allospecificity) have been shown to suppress alloimmune responses more effectively than polyclonal Tregs (4, 17-19, 31-34). However, the potential of CD4$^+$ Tregs is limited as they are MHC class II-restricted thus activated primarily by professional APCs. CARs recognise their target antigen in an MHC-independent manner and as such, can confer specificity for donor MHC class I, an alloantigen ubiquitously expressed on tissue parenchyma throughout an allograft.

In this study, we selected HLA-A2 as a target antigen due to its comparatively high prevalence (>40%) in UK donors (63). The scFv used to construct the HLA-A2-specific CAR cross-reacts with HLA-A28 and HLA-A68 (50). CARs which cross-react with various HLA alleles can be used in a wide variety of donor-recipient combinations thus we believe that generating a library of HLA class I-specific CARs using cross-reactive scFvs will allow for an efficient adaptation into the clinic. Furthermore, we demonstrated that these CARs can be efficiently delivered into human Tregs by lentiviral transduction which is currently employed clinically to deliver CD19-specific CARs into Teffs for the treatment of CLL (37, 38). Progress based on the CRISPR/Cas9 system may make more directed and safer gene delivery accessible in the near future (33).

CAR Tregs demonstrably protected HLA-A2$^+$ human skin grafts more effectively than polyclonal Tregs. However, interesting results were also obtained for the ΔCAR Tregs. These cells exhibited a

favoured migration and retention in HLA-A2$^+$ target tissues which enabled the elicitation of greater graft protection than polyclonal Tregs. However, in terms of CD31$^+$ blood vessel integrity, the protection offered by the ΔCAR Tregs was not as great as the CAR Tregs. These findings suggested that the Treg localisation was an important factor in determining the protection offered, particularly as TCR-mediated direct allorecognition could facilitate activation of these cells in the graft. However, to exploit the full potential of CAR technology, a functional CAR which activated Tregs in the presence of HLA-A2 was required.

Although CARs have principally been used to generate cancer-specific Teffs, studies investigating the therapeutic potential of CAR Tregs have been performed. Very recently, the efficacy of human CAR Tregs was demonstrated in the prevention of xeno-GvHD (49). Furthermore, in pre-clinical models of colitis (16, 44, 45) and multiple sclerosis (46), CAR Tregs were found to migrate to locations where their cognate antigen was expressed and suppress undesired immune responses more effectively than polyclonal Tregs. Similarly, we have shown that CAR Tregs redirected towards HLA-A2 preferentially transmigrate through alloantigen-expressing endothelial cells and exhibit a favoured homing and retention in allografts. These observations suggest a clinical potential for CAR Tregs outside of the transplant field, particularly in light of ongoing clinical trials which are assessing the safety and efficacy of polyclonal Treg therapy for the treatment of Type I diabetes (NCT01210664) (27), lupus erythematosus (NCT02428309) and uveitis (NCT02494492).

In conclusion, polyclonal Treg therapy is currently being investigated clinically by us and others as a means of limiting graft rejection. However, to avoid the risk of pan-immunosuppression and provide a tailored therapy, the successful generation and expansion of alloantigen-specific Tregs is required. We demonstrated that clinically-applicable CAR technology may be used to generate donor antigen-specific Tregs which suppress alloimmune responses, providing a future direction for Treg therapy in the pursuit of transplant tolerance in solid organ transplantation.

ACKNOWLEDGMENTS

DISCLOSURE

The authors of this manuscript have no conflicts of interest to disclose as described by the *American Journal of Transplantation*.

FIGURE LEGENDS

Figure 1: CD4⁺CD25⁻ T cells expressing the full-length CAR were activated in the presence of HLA-A2⁺ cells. A-B: Schematic diagrams detailing the components of the CAR genes. A CAR-eGFP fusion protein was generated consisting of a HLA-A2-specific scFv (white), a CD28 hinge/transmembrane (TM) domain (grey), a CD28/CD3ζ signalling domain (light grey) and an eGFP reporter gene (grey dots). A control CAR (ΔCAR) comprising the same elements but no signalling domain was also generated. **C**: Transduction efficiency of CD4⁺CD25⁻ Teffs, prior to cell sorting, as determined by flow

cytometry analysing eGFP expression. Data is representative of 4 individual experiments. **D**: Flow cytometry histogram plots showing the expression of HLA class I, HLA-DR and HLA-A2 (BB7.2 or REA142 clone) by MCF-7 (solid line) and T-47D (dotted line), compared to an isotype control (solid grey). **E**: Macroscopic images of MCF-7 and T-47D monolayers following overnight co-culture with untransduced (UN-TDX), CAR or ΔCAR T cells. Representative data of 4 individual experiments. **F**: Quantification of MCF-7 (HLA-A2[+], black) and T-47D (HLA-A2[−], grey) viability following overnight co-culture with untransduced, CAR or ΔCAR T cells as measured by MTT assay. Percent viability is relative to monolayers cultured alone. IL-2 (**G**) and IFNγ (**H**) production by the T cells during co-culture with cell monolayers, as measured by ELISA. Data shown is mean ± SEM pooled from 4 individual experiments and significance was determined by two-tailed paired Student's t-test where *=*p*<0.05 and ****=*p*<0.0001. ND = not detected.

Figure 2: **Human CD4^{+}CD25^{+} Tregs maintained their phenotype and function following CAR lentiviral transduction and cell sorting. A**: Timeline showing production of human CAR Tregs used for experimentation. **B**: Representative flow cytometry data showing the proportion of Tregs which were successfully transduced (eGFP expression) and the proportion of cells co-expressing the CAR/ΔCAR construct on the cell surface (c-Myc expression) immediately before and after eGFP[+] cell sorting. **C**: Representative flow cytometry data showing the recognition of a HLA-A2 or HLA-B7 (irrelevant)-based dextramer by untransduced, CAR and ΔCAR Tregs. **D**: Activation of untransduced, CAR and ΔCAR Tregs following co-culture with HLA-A2[+] APCs (solid line), HLA-A2[−] APCs (dotted line) or no APCs (solid grey). Tregs were co-cultured with K562 cells or B-LCLs as APCs for 18 hours at a 4:1 Treg:APC ratio after which Treg activation was measured by CD69 expression. K562s were stably transfected to express either HLA-A2 or HLA-A1. SPO (HLA-A2[+]) and BM21 (HLA-A2[−]) B-LCLs were used. Data shown is representative of 2 individual experiments. **E**: Pooled flow cytometry data comparing the expression of typical Treg markers by untransduced (black), CAR (light grey) and ΔCAR

(dark grey) Tregs. Data shown is mean ± SD pooled from 5 individual experiments. **F**: Pooled flow cytometry data comparing the expression of select skin, gut and secondary lymphoid organ homing receptors by untransduced (black), CAR (light grey) and ΔCAR (dark grey) Tregs. Data shown is mean ± SD pooled from 5 individual experiments. **G**: Polyclonal suppression assay comparing the suppressive capacity of untransduced (black line), CAR (light grey line) and ΔCAR (dark grey line) Tregs. Tregs and autologous Teffs activated in a polyclonal manner were co-cultured at differing ratios for 5 days after which Teff proliferation was measured by CellTrace Violet dilution. Data is expressed as percentage of inhibition of responder Teff proliferation, relative to Teffs cultured alone. Data shown is mean ± SEM pooled from 5-6 individual experiments.

Figure 3: **Human CAR Tregs functioned more effectively in the presence of HLA-A2 without eliciting cytotoxicity.** The suppressive capacity of untransduced (**A**), CAR (**B**) and ΔCAR (**C**) Tregs in the presence of HLA-A2$^+$ B-LCLs (black line) or HLA-A2$^-$ B-LCLs (grey line). Data shown is mean ± SEM pooled from 5 individual experiments. **D**: Quantification of MCF-7 (black) and T-47D (grey) viability following overnight co-culture with untransduced, CAR or ΔCAR Tregs as measured by MTT assay. Percent viability is relative to monolayers cultured alone. IFNγ (**E**) and IL-10 (**F**) production by the Tregs during co-culture with cell monolayers, as measured by ELISA. Data shown is mean ± SEM pooled from 3-4 individual experiments. Significance was determined by two-tailed paired Student's t-test where *=$p<0.05$. ND = not detected. **G**: Transmigratory capacity of CAR (black) and ΔCAR (grey) Tregs across IFNγ pre-treated HLA-A2$^-$ and HLA-A2$^+$ HUVEC endothelial cell monolayers. Data shown represents the percentage of CAR and ΔCAR Tregs which transmigrated, relative to untransduced (UN-TDX) Tregs. Data shown in mean ± SEM pooled from 2-6 individual experiment. Significance was determined by two-way ANOVA where *=$p<0.05$.

Figure 4: **Human CAR Tregs inhibited alloimmune-mediated injury of human HLA-A2$^+$ skin grafts more effectively than polyclonal Tregs.** Immunodeficient BRG mice which had received a HLA-A2$^+$ human skin graft were injected with 5x10^6 PBMCs ± 1x10^6 Tregs. Control mice received saline only. Human skin grafts were removed 5 weeks post-injection and cryopreserved sections were fixed and stained either for human CD45/Ki67/DAPI (**A**), CD31/Involucrin/DAPI (**B**) or human FOXP3/human CD3/DAPI (**C**). Images are representative immunofluorescence stains of human skin grafts. Quantification of the number of Ki67$^+$ keratinocytes (**D**), CD31$^+$ cluster size (**E**) and FOXP3:CD3 ratio (**F**) per field of view was performed using NIS Elements and FIJI imaging software (51). Results represent 2-3 mice/group where 4-6 fields of view were quantified per section and data is representative of 2 individual experiments. Significance was determined by one-way ANOVA and the Tukey multiple comparison post-hoc test where *=$p<0.05$, **=$p<0.01$, ***=$p<0.001$ and ****=$p<0.0001$. ns = not significant.

SUPPORTING INFORMATION

Additional Supporting Information may be found in the online version of this article.

Figure S1: **Isolation purity of human CD4$^+$CD25$^+$ Tregs. A**: Following isolation, Tregs were co-stained for CD4 (OKT4) and CD25 (4E3) and the purity was determined by flow cytometry to be 96.2%. Data is representative of 15 individual experiments. **B**: Following live/dead discrimination, cells were assessed for expression of the following markers by flow cytometry: CD4 (OKT4), CD25 (4E3), CD127 (A019D5), FOXP3 (PCH101), CTLA-4 (BNI3) and CD39 (eBioA1). Data shown is mean ± SD pooled from 6 individual experiments.

Figure S2: Proliferation of Tregs in the presence of HLA-A2$^+$ and HLA-A2$^−$ APCs. Proliferation of untransduced (red), CAR (blue) and ΔCAR (green) Tregs following co-culture with HLA-A2$^+$ and HLA-A2$^−$ APCs. Tregs were co-cultured with K562 cells (**A**) or B-LCLs (**B**) as APCs for 72 hours at a 1:1 ratio. Treg proliferation was measured by ^{3}H-thymidine incorporation and is shown in cpm (counts per

minute) where the cpm of APCs cultured alone was subtracted. K562s were stably transfected to express either HLA-A2 or HLA-A1. SPO (HLA-A2$^+$) and BM21 (HLA-A2$^-$) B-LCLs were used. Data shown is mean ± SD and is representative of 2 individual experiments. Significance was determined by two-tailed paired Student's t-test where *=p<0.05. ns = not significant.

Figure S3: Detailed phenotypic analysis of transduced human Tregs. Representative flow cytometry plots comparing the expression of typical Tregs markers (**A**) and various homing receptors (**B**) by untransduced (UN-TDX; red line) CAR (blue line) and ΔCAR (green line) Tregs. Isotype control staining is shown in solid grey. Data shown is representative of 5 individual experiments.

Figure S4: Schematic diagrams detailing the experimental design of the human skin xenograft transplant experiments. A: Human skin from HLA-A2$^+$ donors was transplanted onto recipient immunodeficient BRG mice and allowed to engraft for 5-6 weeks. These mice were then injected intravenously with allogeneic HLA-A2$^-$ PBMCs with or without autologous *ex vivo*-expanded Tregs. Mice were sacrificed 5 weeks following PBMC infusion and skin grafts were monitored histologically for changes in skin morphology and cell infiltration. **B**: Timeline showing when mice were transplanted with human skin, injected with allogeneic PBMCs ± Tregs and sacrificed to analyse skin graft histology.

Figure S5: HLA-A2 expression on skin-derived cells. Small explants of human skin were tested for HLA-A2 expression by flow cytometry prior to transplantation. Cells acquired by treating explants with collagenase for 1 hour were stained with two separate HLA-A2-specific antibody clones (BB7.2 and REA142 denoted by blue and green lines, respectively). HLA-A2-expression was compared to cells stained with an isotype control, shown in solid grey.

Figure S6: Mice transplanted with human skin allografts did not lose weight following PBMC transfer. A: Transplanted mice injected with allogeneic PBMCs ± Tregs showed no signs of graft-

versus-host disease and no weight loss. **B**: Representative haematoxylin/eosin stains of skin grafts stained in Figure 4.

REFERENCES

1.   Booth AJ, Grabauskiene S, Wood SC, Lu G, Burrell BE, Bishop DK. IL-6 promotes cardiac graft rejection mediated by CD4+ cells. Journal of immunology. 2011;187(11):5764-71.

2.   Pasquet L, Douet JY, Sparwasser T, Romagnoli P, van Meerwijk JP. Long-term prevention of chronic allograft rejection by regulatory T-cell immunotherapy involves host Foxp3-expressing T cells. Blood. 2013;121(21):4303-10.

3.   Sagoo P, Lombardi G, Lechler RI. Relevance of regulatory T cell promotion of donor-specific tolerance in solid organ transplantation. Front Immunol. 2012;3:184.

4.   Tsang JY, Tanriver Y, Jiang S, Leung E, Ratnasothy K, Lombardi G, et al. Indefinite mouse heart allograft survival in recipient treated with CD4(+)CD25(+) regulatory T cells with indirect allospecificity and short term immunosuppression. Transpl Immunol. 2009;21(4):203-9.

5.   Rogers NJ, Lechler RI. Allorecognition. Am J Transplant. 2001;1(2):97-102.

6.   Game DS, Lechler RI. Pathways of allorecognition: implications for transplantation tolerance. Transpl Immunol. 2002;10(2-3):101-8.

7.   Safinia N, Leech J, Hernandez-Fuentes M, Lechler R, Lombardi G. Promoting transplantation tolerance; adoptive regulatory T cell therapy. Clin Exp Immunol. 2013;172(2):158-68.

8.   Meier-Kriesche HU, Kaplan B. The search for CNI-free immunosuppression: no free lunch. Am J Transplant. 2011;11(7):1355-6.

9.   Wojciechowski D, Vincenti F. Tofacitinib in kidney transplantation. Expert Opin Investig Drugs. 2013;22(9):1193-9.

10.   Burgos D, Gonzalez-Molina M, Ruiz-Esteban P, Gutierrez C, Rodriguez MA, Fuentes L, et al. Rate of long-term graft loss has fallen among kidney transplants from cadaveric donors. Transplant Proc. 2012;44(9):2558-60.

11.   Gruessner RW, Gruessner AC. The current state of pancreas transplantation. Nat Rev Endocrinol. 2013;9(9):555-62.

12.   Sakaguchi S, Wing K, Onishi Y, Prieto-Martin P, Yamaguchi T. Regulatory T cells: how do they suppress immune responses? Int Immunol. 2009;21(10):1105-11.

13.   Barzaghi F, Passerini L, Bacchetta R. Immune dysregulation, polyendocrinopathy, enteropathy, x-linked syndrome: a paradigm of immunodeficiency with autoimmunity. Front Immunol. 2012;3:211.

14.   Katoh H, Zheng P, Liu Y. FOXP3: genetic and epigenetic implications for autoimmunity. J Autoimmun. 2013;41:72-8.

15.   Miyara M, Gorochov G, Ehrenstein M, Musset L, Sakaguchi S, Amoura Z. Human FoxP3+ regulatory T cells in systemic autoimmune diseases. Autoimmun Rev. 2011;10(12):744-55.

16.   Elinav E, Waks T, Eshhar Z. Redirection of regulatory T cells with predetermined specificity for the treatment of experimental colitis in mice. Gastroenterology. 2008;134(7):2014-24.

17.   Tsang JY, Tanriver Y, Jiang S, Xue SA, Ratnasothy K, Chen D, et al. Conferring indirect allospecificity on CD4+CD25+ Tregs by TCR gene transfer favors transplantation tolerance in mice. J Clin Invest. 2008;118(11):3619-28.

18.   Golshayan D, Jiang S, Tsang J, Garin MI, Mottet C, Lechler RI. In vitro-expanded donor alloantigen-specific CD4+CD25+ regulatory T cells promote experimental transplantation tolerance. Blood. 2007;109(2):827-35.

19.   Sagoo P, Ali N, Garg G, Nestle FO, Lechler RI, Lombardi G. Human regulatory T cells with alloantigen specificity are more potent inhibitors of alloimmune skin graft damage than polyclonal regulatory T cells. Sci Transl Med. 2011;3(83):83ra42.

20.   Krustrup D, Madsen CB, Iversen M, Engelholm L, Ryder LP, Andersen CB. The number of regulatory T cells in transbronchial lung allograft biopsies is related to FoxP3 mRNA levels in bronchoalveolar lavage fluid and to the degree of acute cellular rejection. Transpl Immunol. 2013.

21.   Krystufkova E, Sekerkova A, Striz I, Brabcova I, Girmanova E, Viklicky O. Regulatory T cells in kidney transplant recipients: the effect of induction immunosuppression therapy. Nephrol Dial Transplant. 2012;27(6):2576-82.
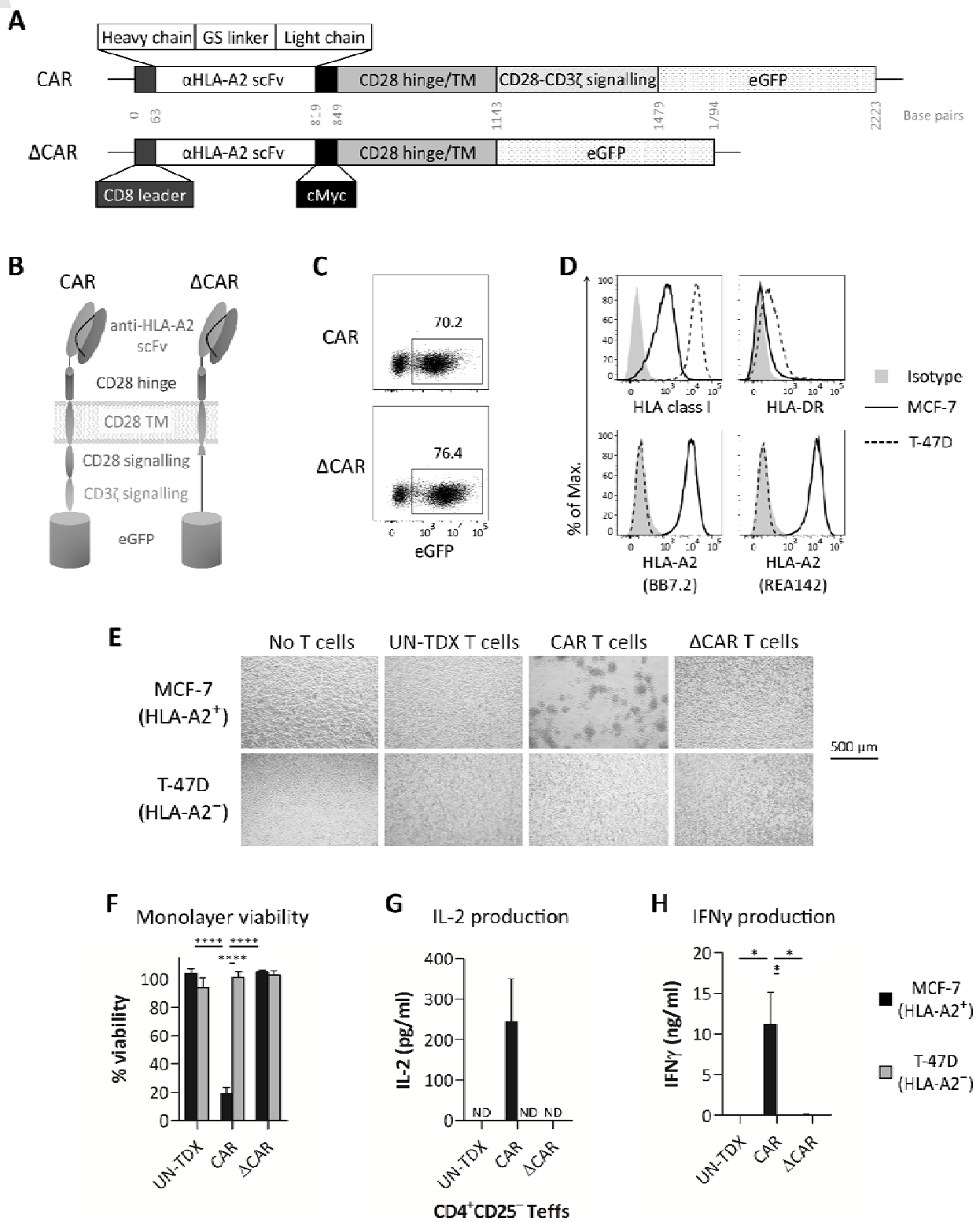
22.   Louis S, Braudeau C, Giral M, Dupont A, Moizant F, Robillard N, et al. Contrasting CD25hiCD4+T cells/FOXP3 patterns in chronic rejection and operational drug-free tolerance. Transplantation. 2006;81(3):398-407.

23.   Di Ianni M, Falzetti F, Carotti A, Terenzi A, Castellino F, Bonifacio E, et al. Tregs prevent GVHD and promote immune reconstitution in HLA-haploidentical transplantation. Blood. 2011;117(14):3921-8.

24.   Brunstein CG, Miller JS, Cao Q, McKenna DH, Hippen KL, Curtsinger J, et al. Infusion of ex vivo expanded T regulatory cells in adults transplanted with umbilical cord blood: safety profile and detection kinetics. Blood. 2011;117(3):1061-70.

25.   Trzonkowski P, Bieniaszewska M, Juscinska J, Dobyszuk A, Krzystyniak A, Marek N, et al. First-in-man clinical results of the treatment of patients with graft versus host disease with human ex vivo expanded CD4+CD25+CD127- T regulatory cells. Clin Immunol. 2009;133(1):22-6.

26.   Theil A, Tuve S, Oelschlagel U, Maiwald A, Dohler D, Ossmann D, et al. Adoptive transfer of allogeneic regulatory T cells into patients with chronic graft-versus-host disease. Cytotherapy. 2015;17(4):473-86.

27.   Bluestone JA, Buckner JH, Fitch M, Gitelman SE, Gupta S, Hellerstein MK, et al. Type 1 diabetes immunotherapy using polyclonal regulatory T cells. Sci Transl Med. 2015;7(315):315ra189.

28.   Marek-Trzonkowska N, Mysliwiec M, Dobyszuk A, Grabowska M, Derkowska I, Juscinska J, et al. Therapy of type 1 diabetes with CD4(+)CD25(high)CD127-regulatory T cells prolongs survival of pancreatic islets - results of one year follow-up. Clin Immunol. 2014;153(1):23-30.

29.   Safinia N, Vaikunthanathan T, Fraser H, Thirkell S, Lowe K, Blackmore L, et al. Successful expansion of functional and stable regulatory T cells for immunotherapy in liver transplantation. Oncotarget. 2016.

30.   Afzali B, Edozie FC, Fazekasova H, Scotta C, Mitchell PJ, Canavan JB, et al. Comparison of regulatory T cells in hemodialysis patients and healthy controls: implications for cell therapy in transplantation. Clin J Am Soc Nephrol. 2013;8(8):1396-405.

31.   Putnam AL, Safinia N, Medvec A, Laszkowska M, Wray M, Mintz MA, et al. Clinical grade manufacturing of human alloantigen-reactive regulatory T cells for use in transplantation. Am J Transplant. 2013;13(11):3010-20.

32.   Joffre O, Santolaria T, Calise D, Al Saati T, Hudrisier D, Romagnoli P, et al. Prevention of acute and chronic allograft rejection with CD4+CD25+Foxp3+ regulatory T lymphocytes. Nat Med. 2008;14(1):88-92.

33.   Lee K, Nguyen V, Lee KM, Kang SM, Tang Q. Attenuation of donor-reactive T cells allows effective control of allograft rejection using regulatory T cell therapy. Am J Transplant. 2014;14(1):27-38.

34.   Landwehr-Kenzel S, Issa F, Luu SH, Schmuck M, Lei H, Zobel A, et al. Novel GMP-compatible protocol employing an allogeneic B cell bank for clonal expansion of allospecific natural regulatory T cells. Am J Transplant. 2014;14(3):594-606.

35.   Boardman D, Maher J, Lechler R, Smyth L, Lombardi G. Antigen-specificity using chimeric antigen receptors: the future of regulatory T-cell therapy? Biochem Soc Trans. 2016;44(2):342-8.

36.   Maher J. Immunotherapy of malignant disease using chimeric antigen receptor engrafted T cells. ISRN Oncol. 2012;2012:278093.

37.   Porter DL, Levine BL, Kalos M, Bagg A, June CH. Chimeric antigen receptor-modified T cells in chronic lymphoid leukemia. N Engl J Med. 2011;365(8):725-33.

38.   Kalos M, Levine BL, Porter DL, Katz S, Grupp SA, Bagg A, et al. T cells with chimeric antigen receptors have potent antitumor effects and can establish memory in patients with advanced leukemia. Sci Transl Med. 2011;3(95):95ra73.

39.   Grupp SA, Kalos M, Barrett D, Aplenc R, Porter DL, Rheingold SR, et al. Chimeric Antigen Receptor-Modified T Cells for Acute Lymphoid Leukemia. N Engl J Med. 2013.

40.   Brentjens RJ, Davila ML, Riviere I, Park J, Wang X, Cowell LG, et al. CD19-targeted T cells rapidly induce molecular remissions in adults with chemotherapy-refractory acute lymphoblastic leukemia. Sci Transl Med. 2013;5(177):177ra38.

41.   Till BG, Jensen MC, Wang J, Qian X, Gopal AK, Maloney DG, et al. CD20-specific adoptive immunotherapy for lymphoma using a chimeric antigen receptor with both CD28 and 4-1BB domains: pilot clinical trial results. Blood. 2012;119(17):3940-50.

42.   Kochenderfer JN, Wilson WH, Janik JE, Dudley ME, Stetler-Stevenson M, Feldman SA, et al. Eradication of B-lineage cells and regression of lymphoma in a patient treated with autologous T cells genetically engineered to recognize CD19. Blood. 2010;116(20):4099-102.

43.   Kohn DB, Dotti G, Brentjens R, Savoldo B, Jensen M, Cooper LJ, et al. CARs on track in the clinic. Mol Ther. 2011;19(3):432-8.

44.   Elinav E, Adam N, Waks T, Eshhar Z. Amelioration of colitis by genetically engineered murine regulatory T cells redirected by antigen-specific chimeric receptor. Gastroenterology. 2009;136(5):1721-31.

45.   Blat D, Zigmond E, Alteber Z, Waks T, Eshhar Z. Suppression of murine colitis and its associated cancer by carcinoembryonic antigen-specific regulatory T cells. Mol Ther. 2014;22(5):1018-28.

46.   Fransson M, Piras E, Burman J, Nilsson B, Essand M, Lu B, et al. CAR/FoxP3-engineered T regulatory cells target the CNS and suppress EAE upon intranasal delivery. J Neuroinflammation. 2012;9:112.

47.   Lee JC, Hayman E, Pegram HJ, Santos E, Heller G, Sadelain M, et al. In vivo inhibition of human CD19-targeted effector T cells by natural T regulatory cells in a xenotransplant murine model of B cell malignancy. Cancer Res. 2011;71(8):2871-81.

48.   Jethwa H, Adami AA, Maher J. Use of gene-modified regulatory T-cells to control autoimmune and alloimmune pathology: is now the right time? Clin Immunol. 2014;150(1):51-63.

49.   MacDonald KG, Hoeppli RE, Huang Q, Gillies J, Luciani DS, Orban PC, et al. Alloantigen-specific regulatory T cells generated with a chimeric antigen receptor. J Clin Invest. 2016.

50.   Watkins NA, Brown C, Hurd C, Navarrete C, Ouwehand WH. The isolation and characterisation of human monoclonal HLA-A2 antibodies from an immune V gene phage display library. Tissue Antigens. 2000;55(3):219-28.

51.   Schindelin J, Arganda-Carreras I, Frise E, Kaynig V, Longair M, Pietzsch T, et al. Fiji: an open-source platform for biological-image analysis. Nat Methods. 2012;9(7):676-82.

52.   Krause A, Guo HF, Latouche JB, Tan C, Cheung NK, Sadelain M. Antigen-dependent CD28 signaling selectively enhances survival and proliferation in genetically modified activated human primary T lymphocytes. J Exp Med. 1998;188(4):619-26.

53.   Finney HM, Lawson AD, Bebbington CR, Weir AN. Chimeric receptors providing both primary and costimulatory signaling in T cells from a single gene product. J Immunol. 1998;161(6):2791-7.

54.   Maher J, Brentjens RJ, Gunset G, Riviere I, Sadelain M. Human T-lymphocyte cytotoxicity and proliferation directed by a single chimeric TCRzeta /CD28 receptor. Nat Biotechnol. 2002;20(1):70-5.

55.   Savoldo B, Ramos CA, Liu E, Mims MP, Keating MJ, Carrum G, et al. CD28 costimulation improves expansion and persistence of chimeric antigen receptor-modified T cells in lymphoma patients. J Clin Invest. 2011;121(5):1822-6.

56.   Hombach AA, Kofler D, Hombach A, Rappl G, Abken H. Effective proliferation of human regulatory T cells requires a strong costimulatory CD28 signal that cannot be substituted by IL-2. J Immunol. 2007;179(11):7924-31.

57.   Carlsson B, Forsberg O, Bengtsson M, Totterman TH, Essand M. Characterization of human prostate and breast cancer cell lines for experimental T cell-based immunotherapy. Prostate. 2007;67(4):389-95.

58.   Scotta C, Esposito M, Fazekasova H, Fanelli G, Edozie FC, Ali N, et al. Differential effects of rapamycin and retinoic acid on expansion, stability and suppressive qualities of human CD4(+)CD25(+)FOXP3(+) T regulatory cell subpopulations. Haematologica. 2013;98(8):1291-9.

59.   Cao X, Cai SF, Fehniger TA, Song J, Collins LI, Piwnica-Worms DR, et al. Granzyme B and perforin are important for regulatory T cell-mediated suppression of tumor clearance. Immunity. 2007;27(4):635-46.

60.   Grossman WJ, Verbsky JW, Barchet W, Colonna M, Atkinson JP, Ley TJ. Human T regulatory cells can use the perforin pathway to cause autologous target cell death. Immunity. 2004;21(4):589-601.

61.   Ma L, Cheung KC, Kishore M, Nourshargh S, Mauro C, Marelli-Berg FM. CD31 exhibits multiple roles in regulating T lymphocyte trafficking in vivo. J Immunol. 2012;189(8):4104-11.

62.   Green H, Easley K, Iuchi S. Marker succession during the development of keratinocytes from cultured human embryonic stem cells. Proc Natl Acad Sci U S A. 2003;100(26):15625-30.

63.   Burt C, Cryer C, Fuggle S, Little AM, Dyer P. HLA-A, -B, -DR allele group frequencies in 7007 kidney transplant list patients in 27 UK centres. Int J Immunogenet. 2013;40(3):209-15.
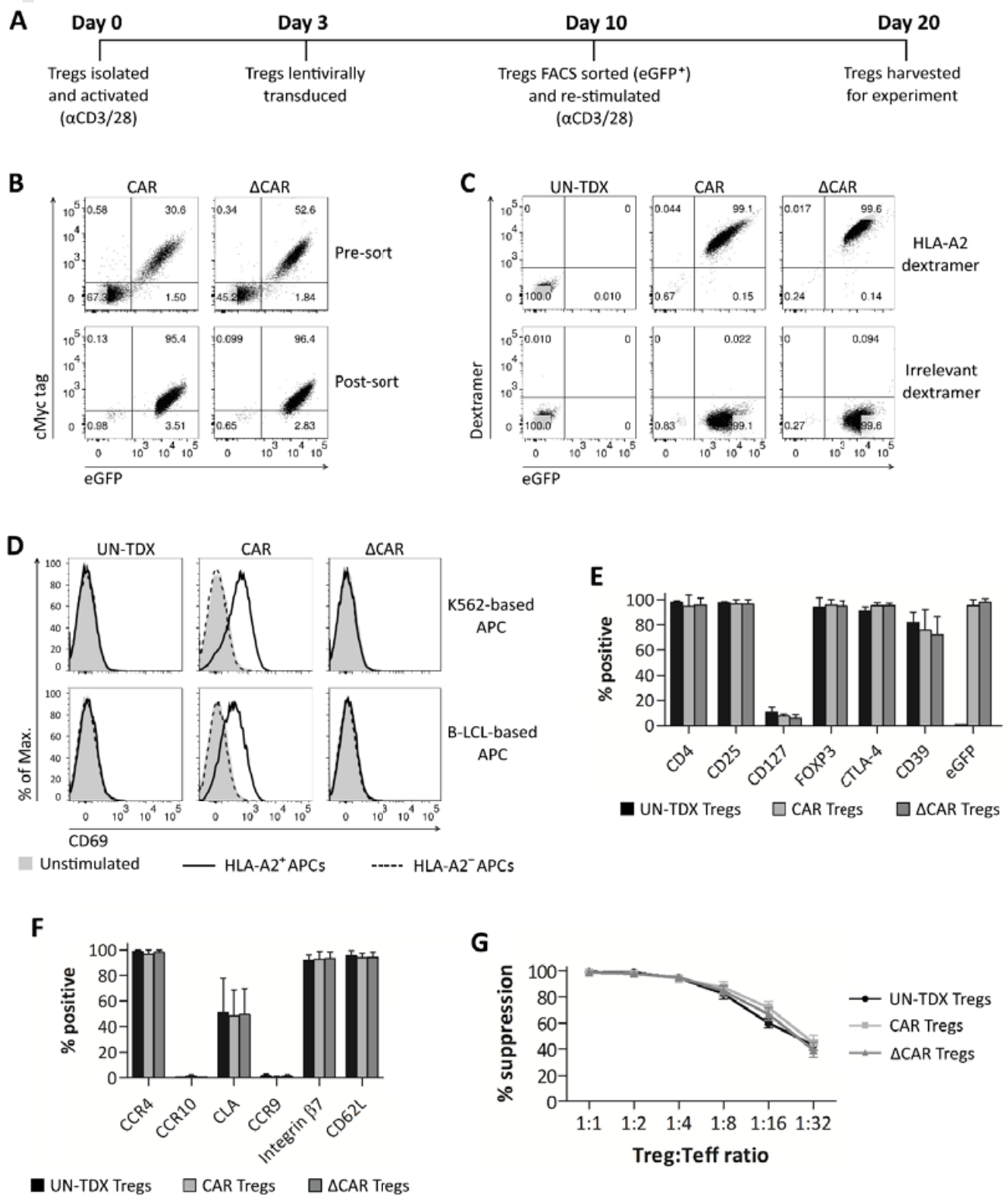
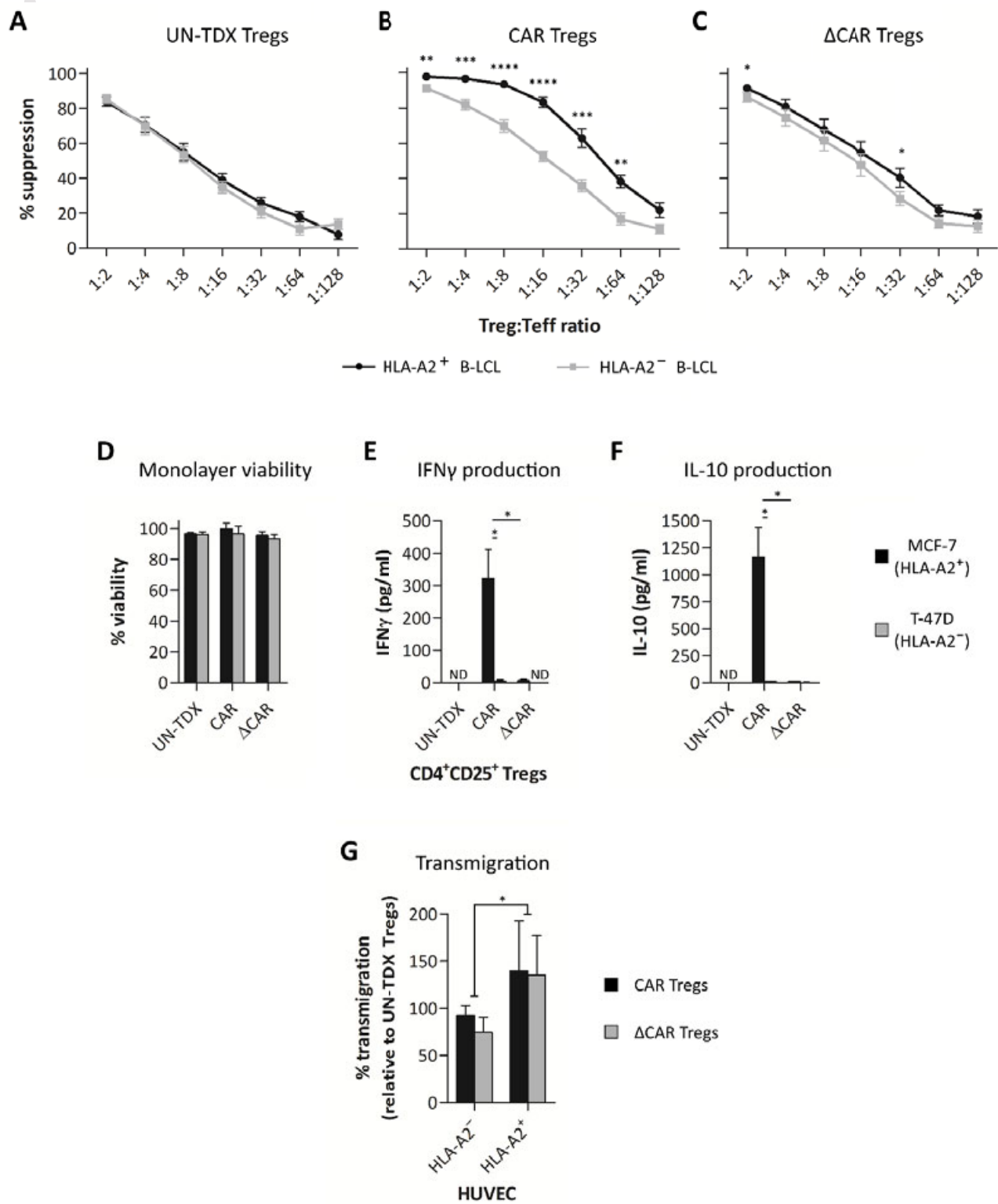**FIGURE 1**

FIGURE 2

FIGURE 3

FIGURE 4

A   CD45 Ki67 DAPI
B   Involucrin
     CD31 DAPI
C   FOXP3 CD3 DAPI

Saline

PBMCs only

PBMCs +
UN-TDX Tregs

PBMCs +
CAR Tregs

PBMCs +
ΔCAR Tregs

200 µm

D   Ki67+ keratinocytes/field

E   CD31+ cluster size/field

F   FOXP3:CD3 ratio/field

- Saline   ■ PBMCs only   ▲ PBMCs + UN-TDX Tregs   ▼ PBMCs + CAR Tregs   ◆ PBMCs + ΔCAR Tregs